Supplementary Information:

p53 activates transcription by directing structural shifts within Mediator

Krista D. Meyer, Shih-Chieh Lin, Carrie Bernecky, Yuefeng Gao, Dylan J. Taatjes
Department of Chemistry and Biochemistry, University of Colorado, Boulder, CO 80309, USA.

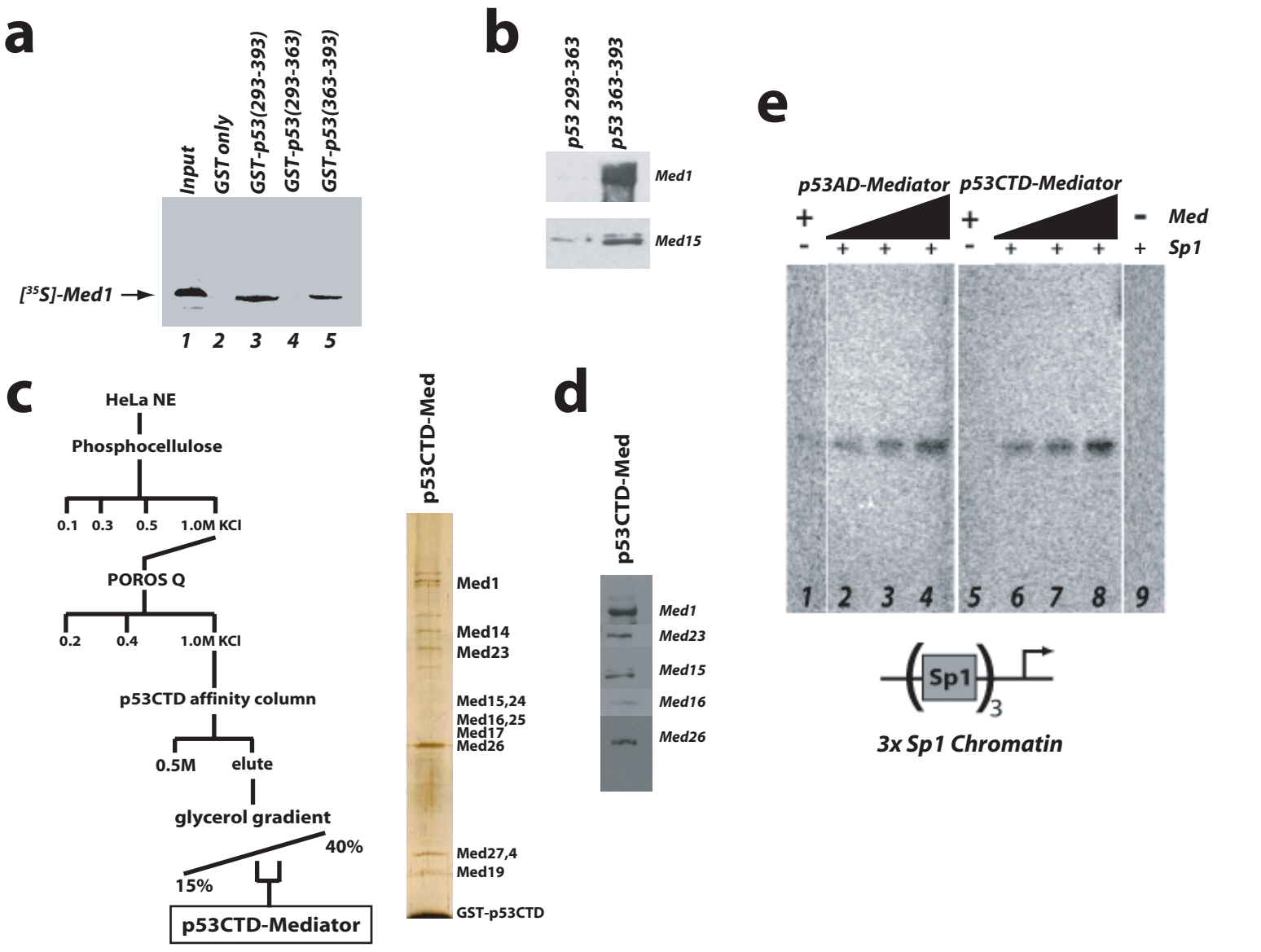

Supplementary Figure 1 | The p53CTD (residues 363-393) binds Med1. (a) An [35S]-labeled Med1 fragment (residues 1234-1406) previously shown to interact with p53[6] was transcribed and translated in vitro using a rabbit reticulocyte lysate. This lysate was then incubated with resin-bound GST (lane 2) or GST fused to various p53 domains as shown. After a series of high-salt (0.5M KCl) washes, bound material was eluted with glutathione and run on a 10% polyacrylamide gel. The [35S]-Med1 fragment was detected by autoradiography. Note only p53 domains containing the 31-residue C-terminal domain (lanes 3 and 5) were capable of binding Med1. **(b)** Immobilized GST-p53 fragments were incubated with HeLa nuclear extract, washed extensively with high-salt buffer, and eluted with glutathione. Eluted material was then probed for the Mediator subunits Med1 and Med15 by western blot. **(c)** Purification protocol and silver-stained gel of Mediator purified with a GST-p53CTD affinity resin. **(d)** The identity of numerous Mediator subunits was confirmed with immunoblotting experiments. **(e) Mediator purified with either p53AD or p53CTD is functionally indistinguishable.** Reconstituted transcription assays on chromatin templates containing Sp1 binding sites. Each reaction (1-9) contained equivalent amounts of chromatin, TFIIA, IIB, IID, IIE, IIF, IIH, pol II, and NTPs. Sp1 and Mediator added as shown. p53AD- and p53CTD-Mediator levels were normalized by comparative silver-staining to ensure similar amounts of Mediator were added in lanes 2-4 versus 6-8. Note that because of low yield with p53CTD-Mediator (e.g. see **Supplementary Fig. 1c**), the amount of Mediator used in these experiments was approximately 5-fold lower than what is normally used in a reconstituted transcription assay. Thus, the absolute levels of transcripts detected by the primer extension assay is lower than a standard experiment. Each experiment (1-9) followed the general timeline outlined in **Figure 2b**. Note that this experiment does not address how alterations in Mediator structure might impact its co-activator function because the promoter contains Sp1 binding sites. Mediator interactions with Sp1 at the promoter likely "normalize" Mediator to a common, Sp1-bound structural state in this assay. Experiments designed to test how Mediator structure impacts its transcriptional activity are shown in **Figure 2c** and **Figure 3a**.

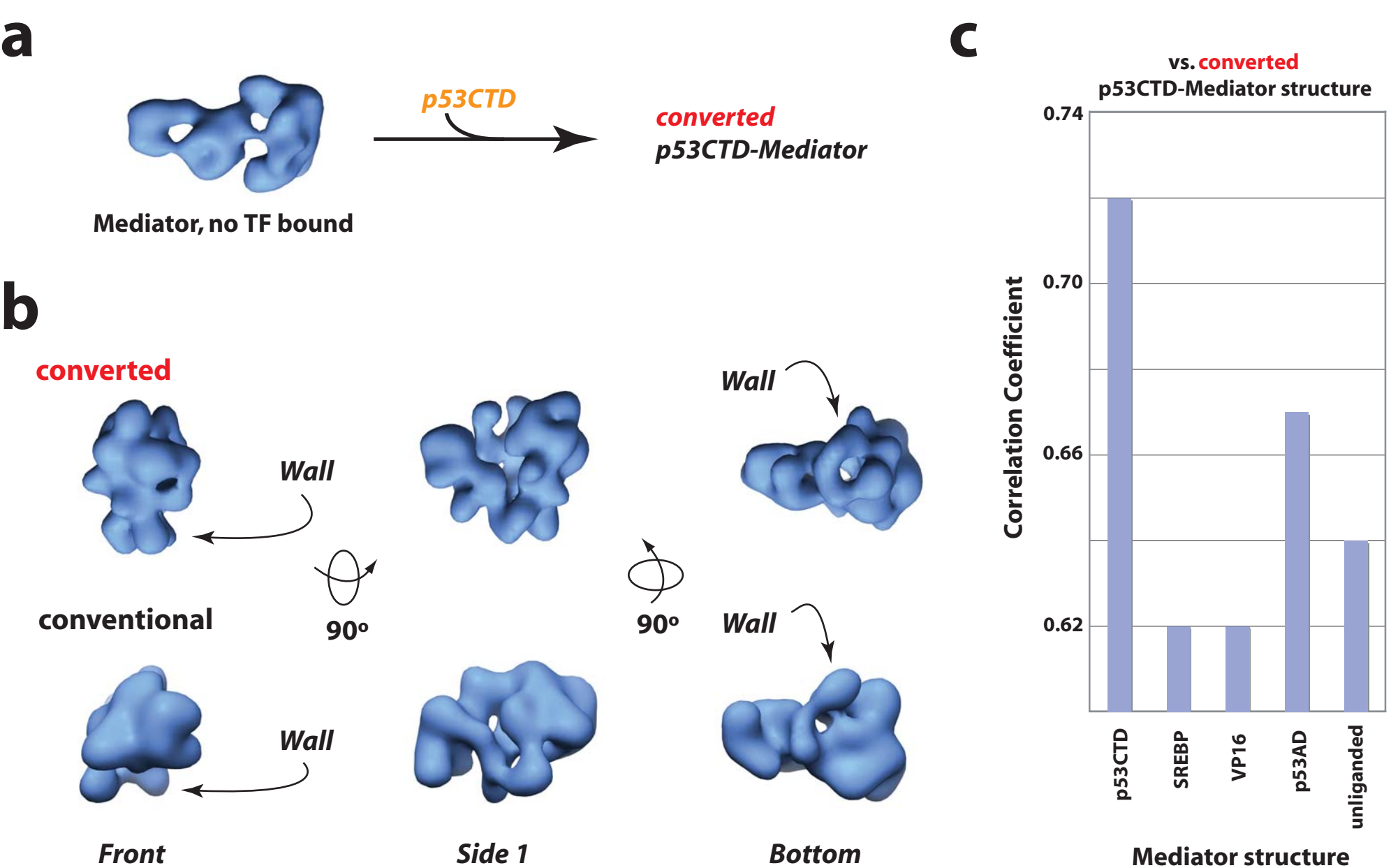

Supplementary Figure 2 | p53CTD binding to unliganded Mediator induces the predicted structural shift. (a) Scheme outlining the experimental protocol. Unliganded Mediator was purified as described[10]. **(b)** Structural comparison of converted p53CTD–Mediator structure and the conventionally-purified p53CTD–Mediator structure. Similar views are shown. The wall domain is noted with an arrow in each structure. Note also the prominent V-shaped density in each structure in the "side 1" orientation. The wall and V-shaped densities are not observed in any other Mediator structure observed to date and therefore are considered specific to p53CTD–Mediator. **(c)** Cross-correlation of various activator-bound Mediator structures (e.g. SREBP, VP16, p53AD) or unliganded Mediator (no activator bound) with the converted p53CTD–Mediator structure. As expected, the converted p53CTD–Mediator structure correlates most highly with the conventionally-purified p53CTD–Mediator structure.

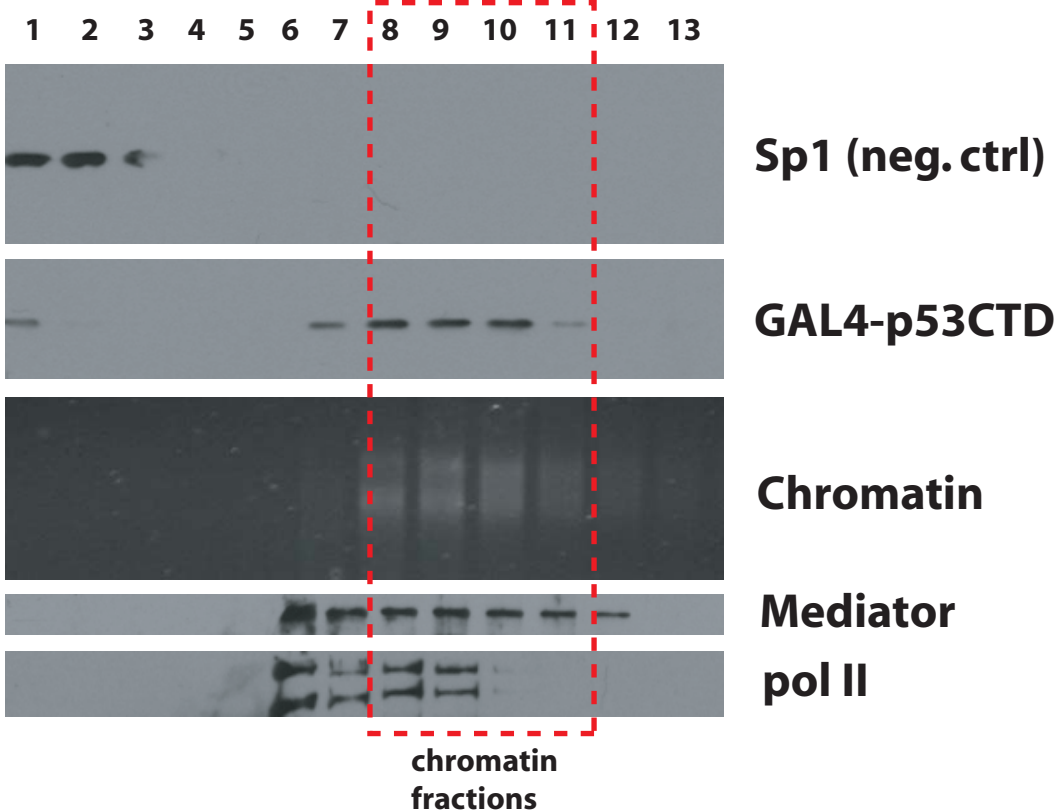

Supplementary Figure 3 | Chromatin sedimentation. PEC assembly on the GAL4 chromatin template was completed as with a reconstituted transcription assay (i.e. as outlined in **Fig. 2b**), followed by separation of free components from chromatin-bound factors by centrifugation, as described[10]. Purified Sp1, which should not bind the GAL4 template, was also added as a negative control. Chromatin was visualized with ethidium bromide staining, whereas GAL4-p53CTD, Sp1, Mediator (Med1), and pol II (Rpb1) were detected via western blot. Note that TFIID and TFIIH were also observed to co-migrate with the chromatin in separate experiments (data not shown). As free complexes, Mediator or pol II will migrate at sedimentation fraction 5-8[10].

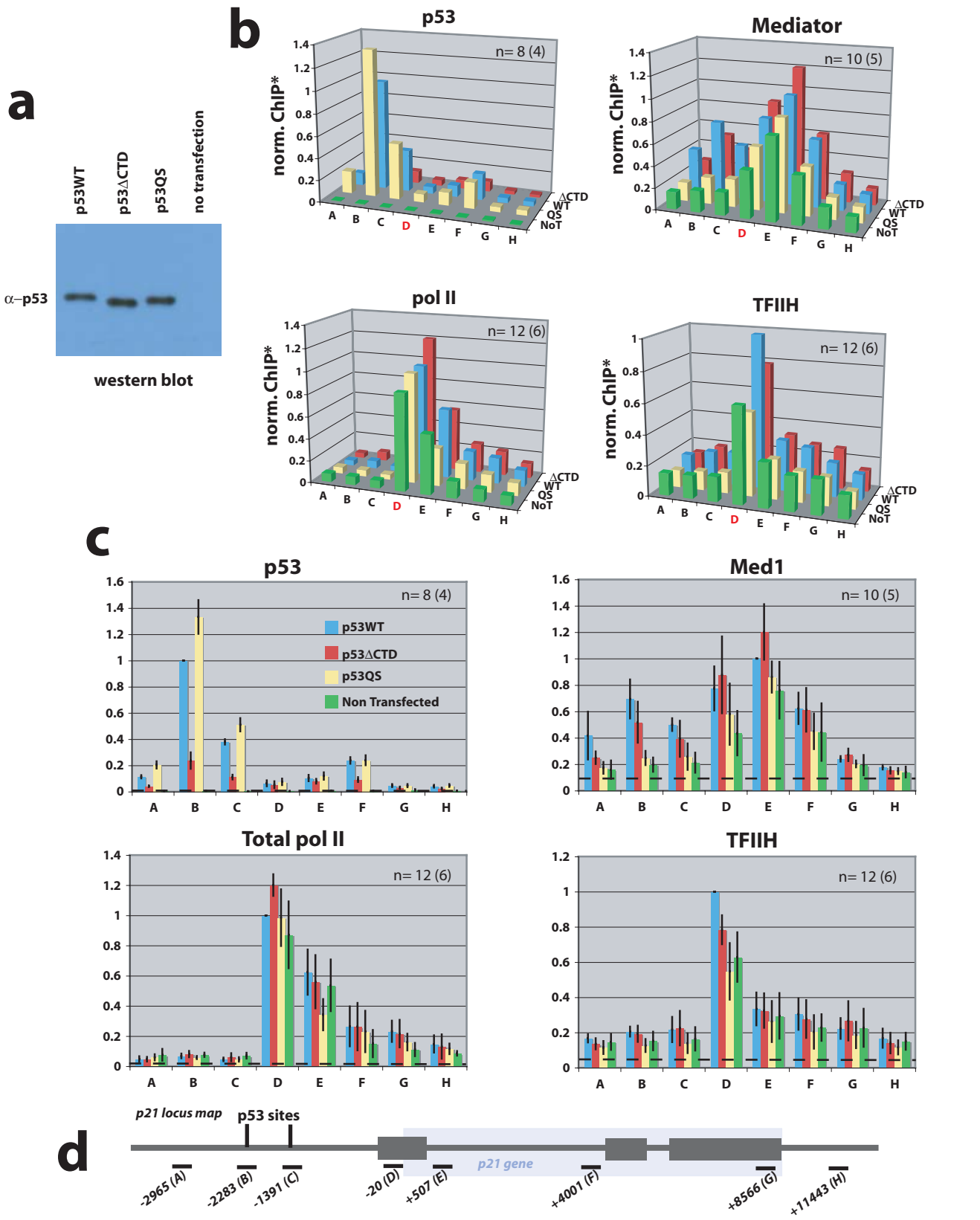

Supplementary Figure 4 | Expression of p53 proteins in p53-null HCT116 cells. (a) Western blots show equivalent levels of each p53 protein (WT p53, p53QS, p53ΔCTD) after transfection. As expected, no endogenous p53 was detectable in these cells. **(b) PEC recruitment at the p21 gene.** Occupancy of various factors was probed along the p21 locus. Note that results are similar to HDM2, including evidence of PEC pre-loading at the promoter (non-transfected controls, green bars). This pre-loading at the p21 gene has been observed in past studies[37]. The probe location in red (**D**) represents the promoter/start site. *ChIP output was normalized to WT p53, typically from primer D. For clarity, error bars are not shown but can be viewed in part **c**, below. **(c)** A different representation of the data from part **b** which shows the s.e.m. for each experiment. The dashed line represents ChIP signal observed in no antibody IP control experiments. **(d)** Schematic of the p21 locus.

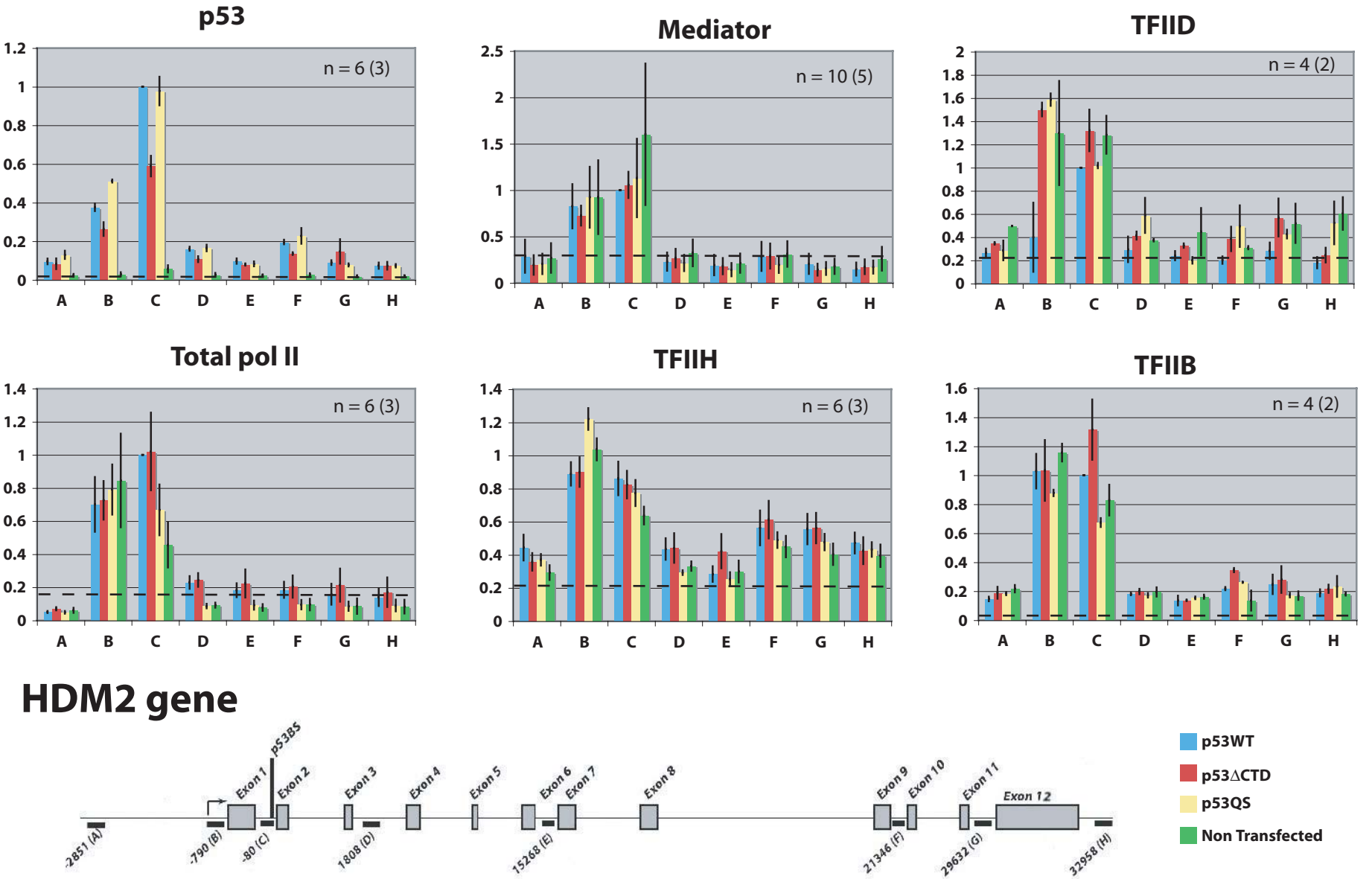

Supplementary Figure 5 | PEC recruitment at the HDM2 gene. A different representation of the data from **Figure 1c,** showing the s.e.m. for each measurement. The dashed line represents ChIP signal observed in no antibody IP control experiments.

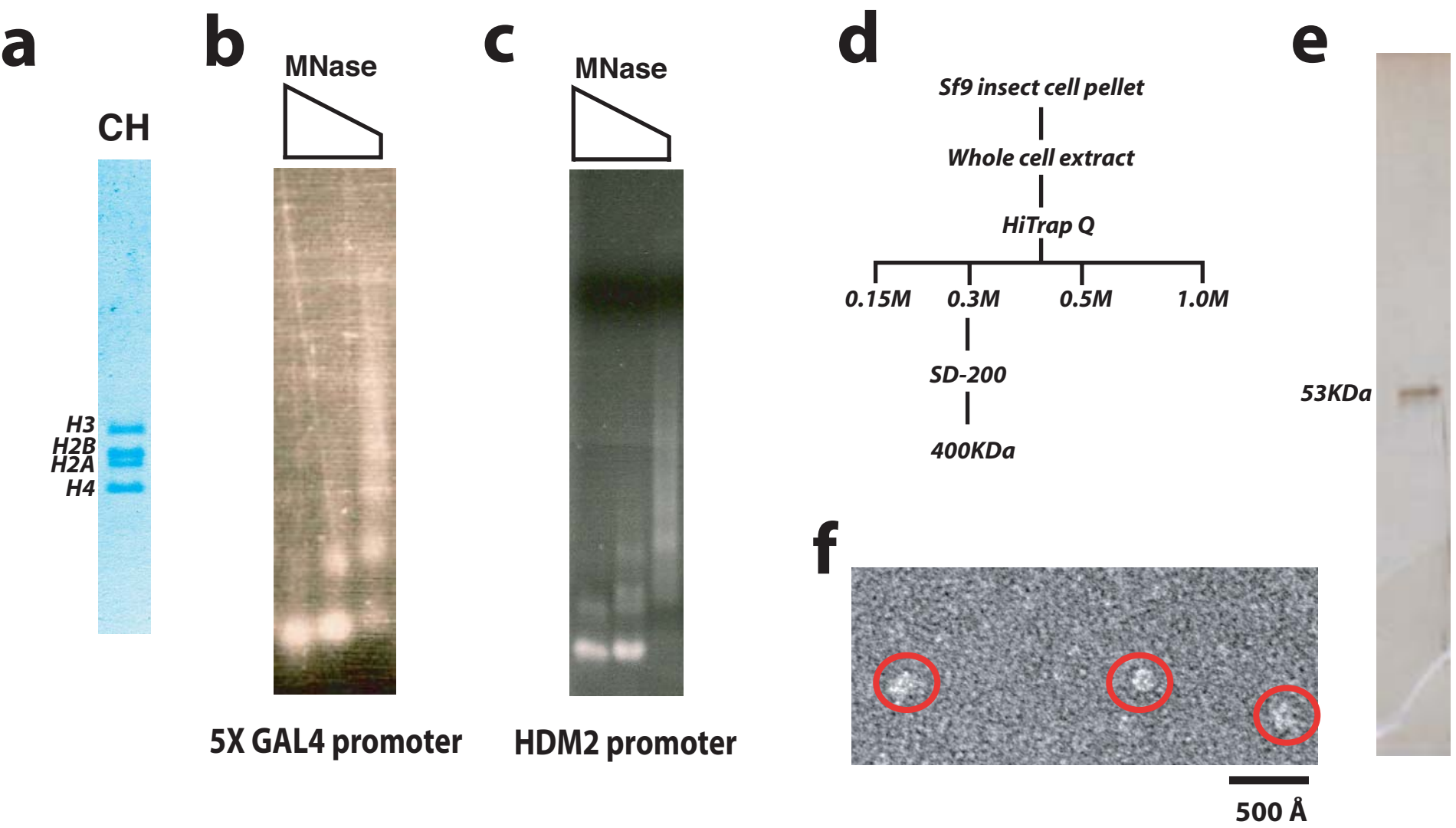

Supplementary Figure 6 | Chromatin assembly. (a) Coomassie-stained gel of purified core histones used for chromatin assembly. **(b)** Micrococcal nuclease digestion of chromatin assembled with supercoiled DNA templates containing tandem GAL4 DNA-binding elements. **(c)** Micrococcal nuclease digestion of chromatin assembled with supercoiled DNA templates containing the native HDM2 promoter. **(d) Purification of wild-type and mutant p53 tetramers.** Purification scheme used to isolate wild-type p53, p53QS, or p53ΔCTD tetramers. **(e)** Silver-stained gel of purified wild-type p53 tetramer sample. Similar results were obtained with p53QS and p53ΔCTD mutant tetramers. **(f)** electron micrograph (50,000x magnification) of purified wild-type p53 tetramer sample. Particles with size and shape consistent with p53 tetramers[8] are circled.

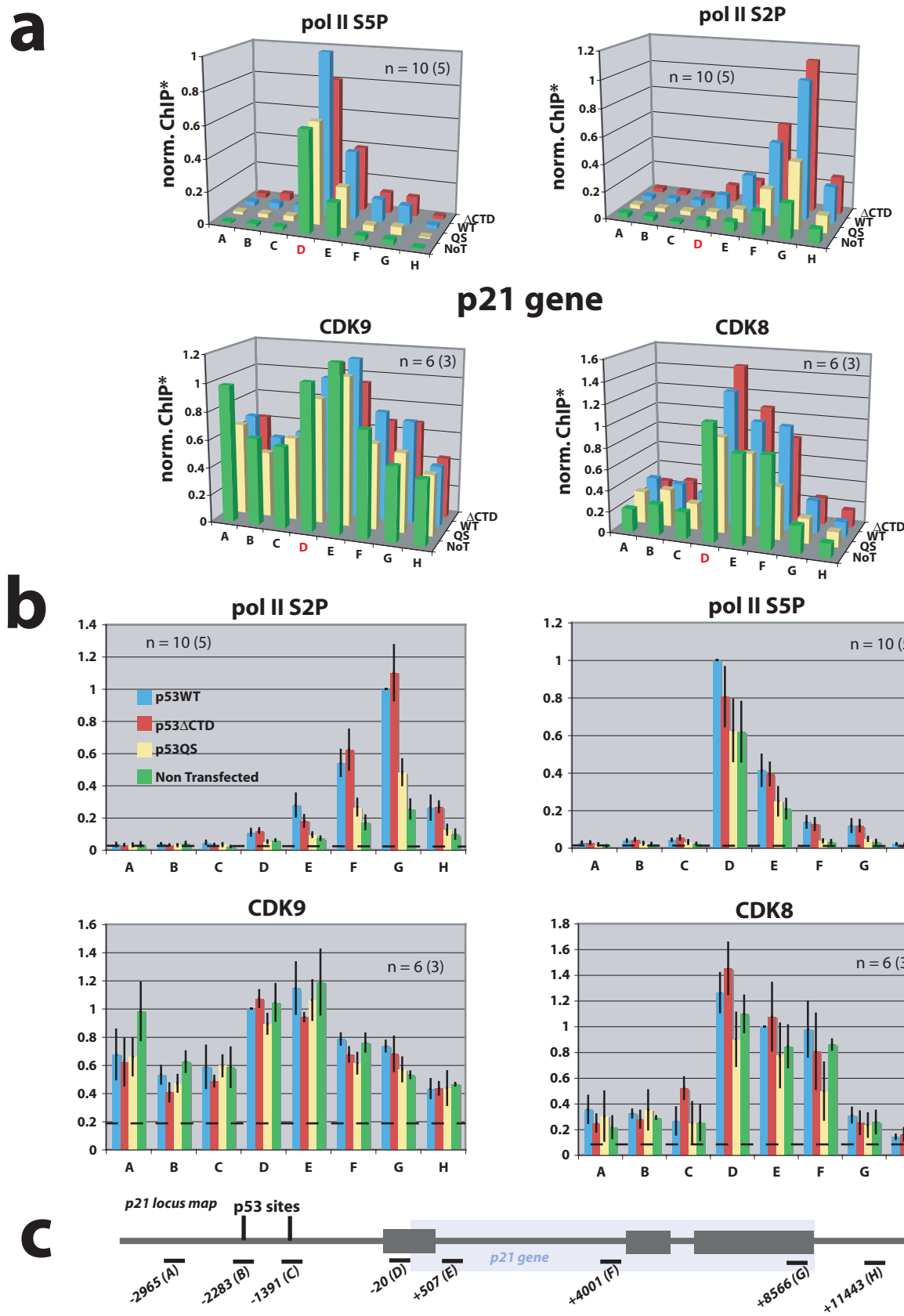

Supplementary Figure 7 | ChIP data and pol II elongation at the p21 gene. **(a)** Occupancy of various phosphorylated forms of pol II (S5P and S2P) and several pol II CTD kinases was probed across the p21 locus. Note that results are similar to HDM2 (**Fig. 4b-e**), and are indicative of pol II elongation in the presence of WT p53 and p53ΔCTD, whereas the ChIP data suggests pol II does not clear the p21 promoter in non-transfected controls or in the presence of p53QS mutant tetramers. The probe location in red (**D**) represents the promoter/start site. *ChIP output was normalized to WT p53, typically from primer D. For clarity, error bars are not shown but can be viewed in part **b**, below. **(b)** A different representation of the data from which shows the s.e.m. for each experiment. The dashed line represents ChIP signal observed in no antibody IP control experiments. **(c)** Map of p21 locus.

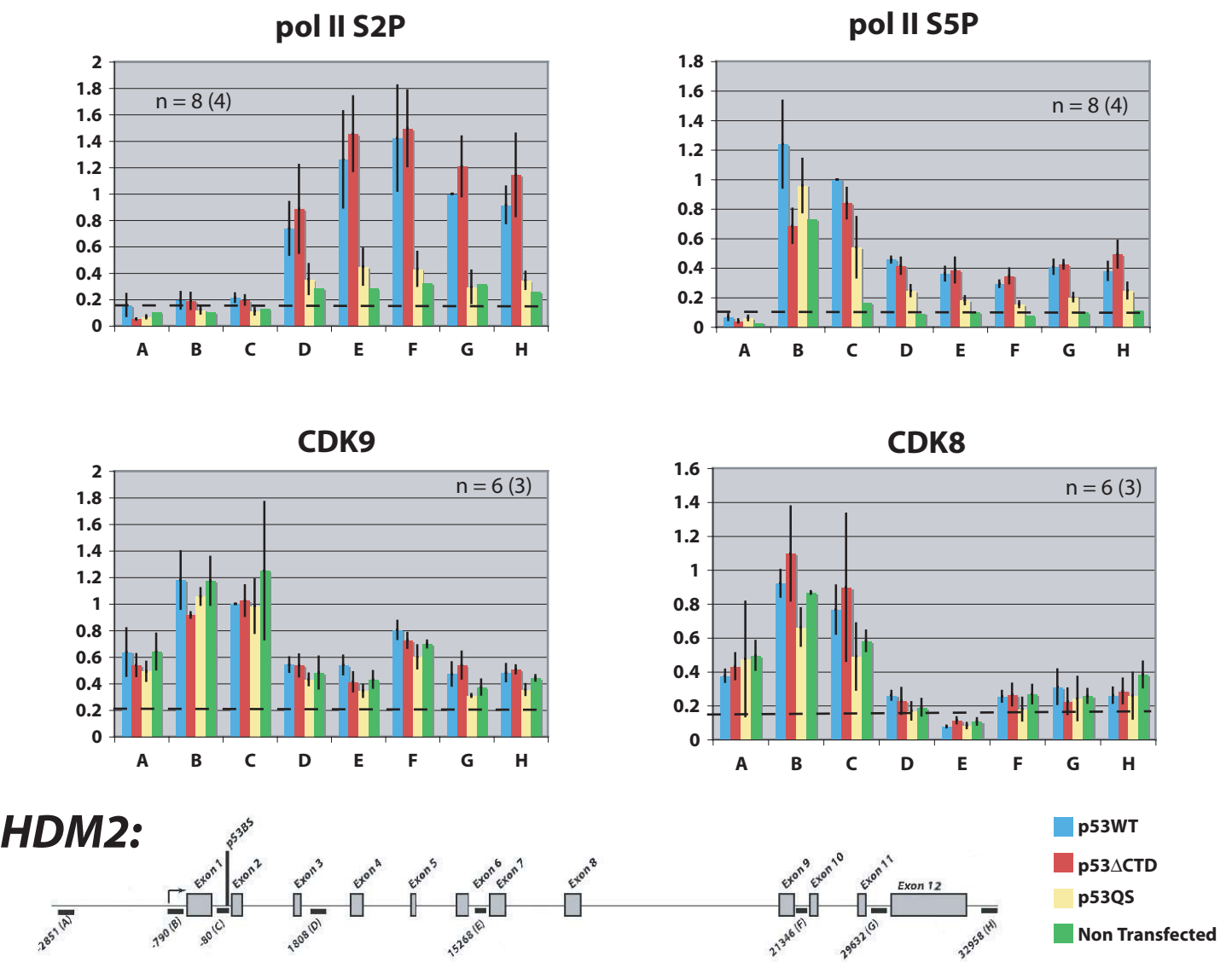

Supplementary Figure 8 | ChIP data at the HDM2 gene. A different representation of the data from **Figure 4b-e**, showing the s.e.m. for each measurement. The dashed line represents ChIP signal observed in no antibody IP control experiments.

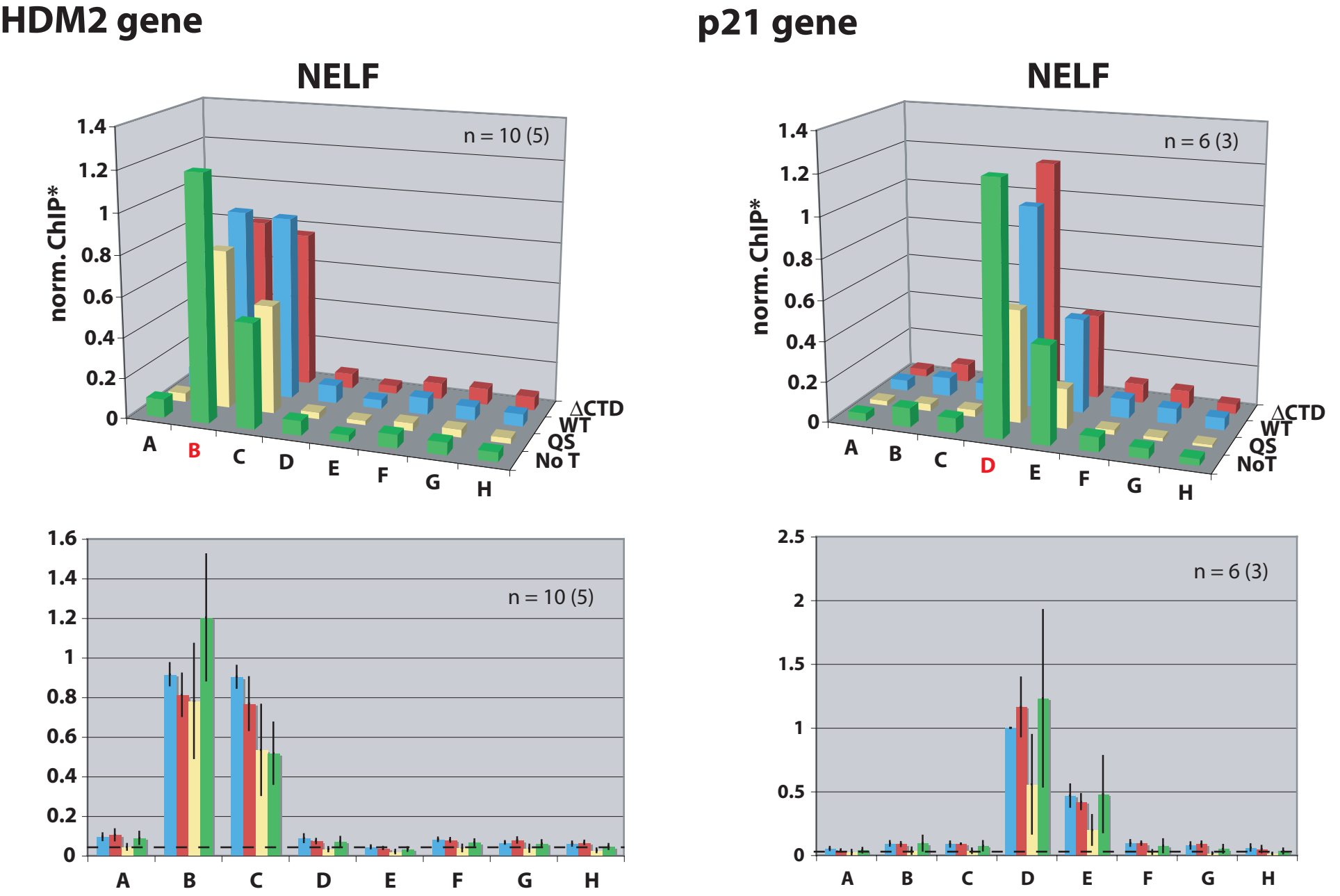

Supplementary Figure 9 | Occupancy of NELF at HDM2 and p21. ChIP data with s.e.m. bars are shown below 3D plots; dashed line represents ChIP signal from no antibody IP controls. The probe location shown in red represents the promoter/start site. *ChIP output was normalized to WT p53, typically from primer C (HDM2) or D (p21).

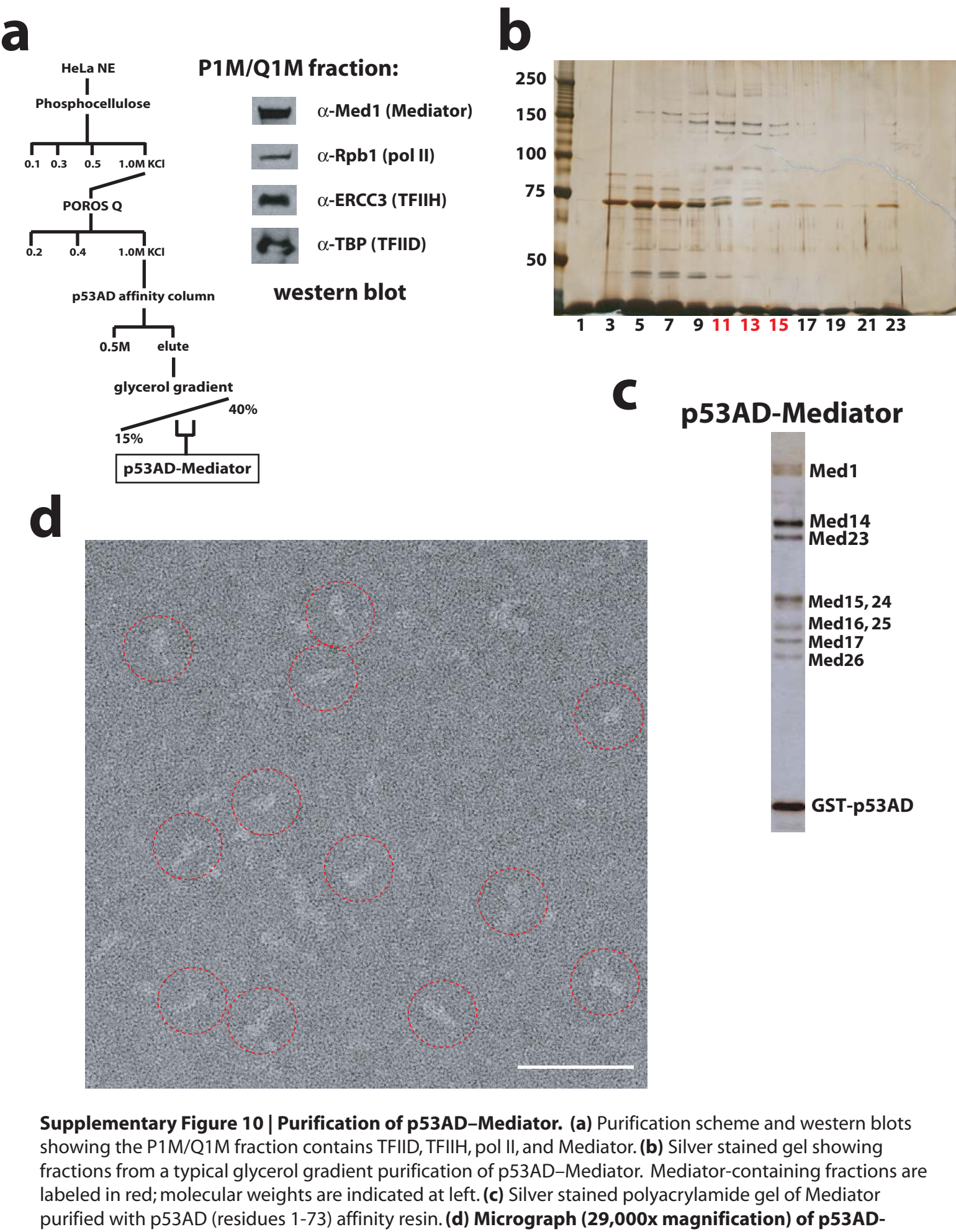

Supplementary Figure 10 | Purification of p53AD–Mediator. **(a)** Purification scheme and western blots showing the P1M/Q1M fraction contains TFIID, TFIIH, pol II, and Mediator. **(b)** Silver stained gel showing fractions from a typical glycerol gradient purification of p53AD–Mediator. Mediator-containing fractions are labeled in red; molecular weights are indicated at left. **(c)** Silver stained polyacrylamide gel of Mediator purified with p53AD (residues 1-73) affinity resin. **(d) Micrograph (29,000x magnification) of p53AD-Mediator sample.** Complexes are circled in red. Bar: 100 nm.

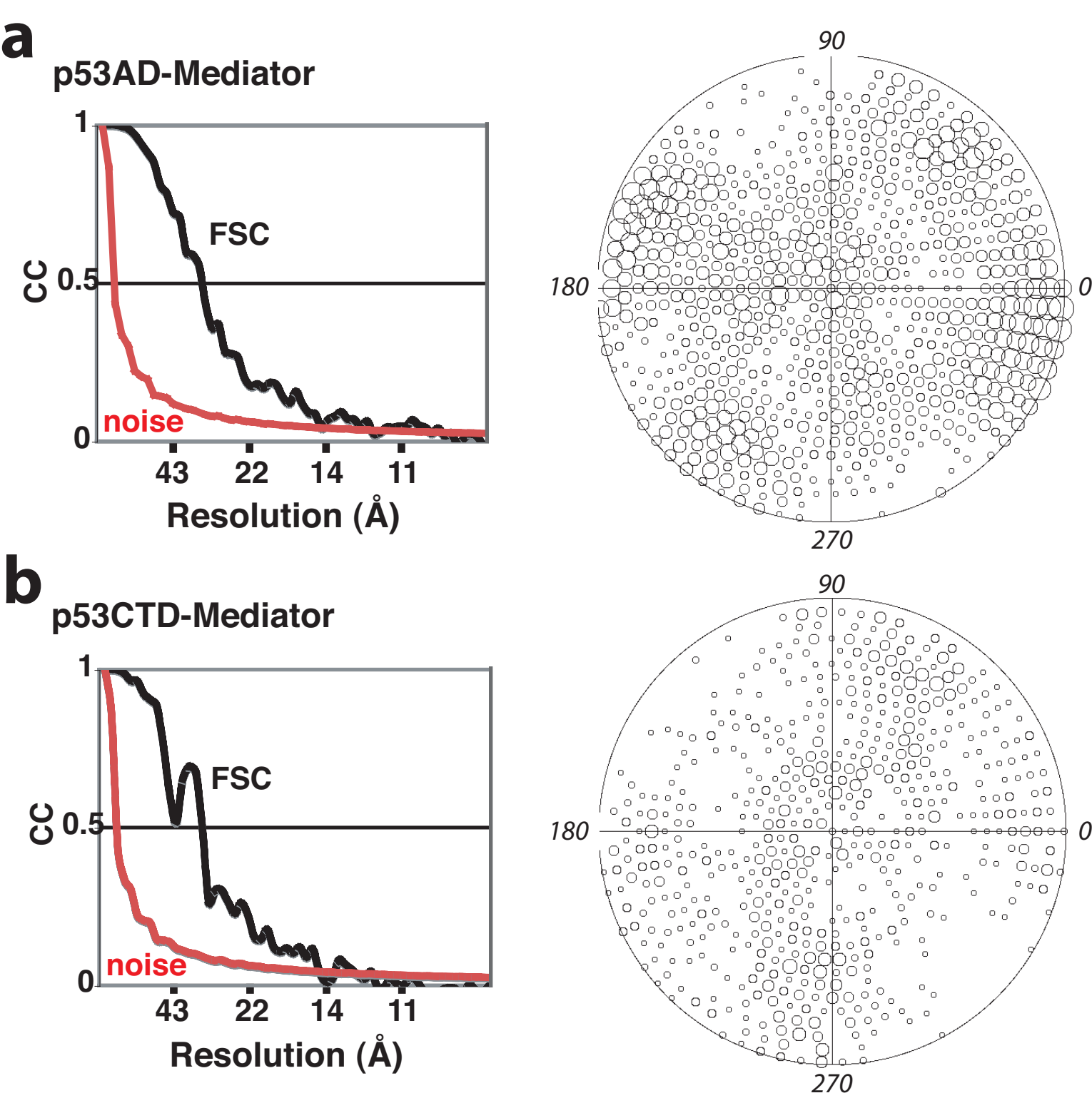

Supplementary Figure 11 | Image processing data for p53AD–Mediator **(a)** and p53CTD-Mediator **(b)** three-dimensional reconstructions. Angular distribution of single-particle images for each data set is shown. Also, Fourier Shell Correlation Coefficient (FSC) and the 3σ noise plotted as a function of resolution.

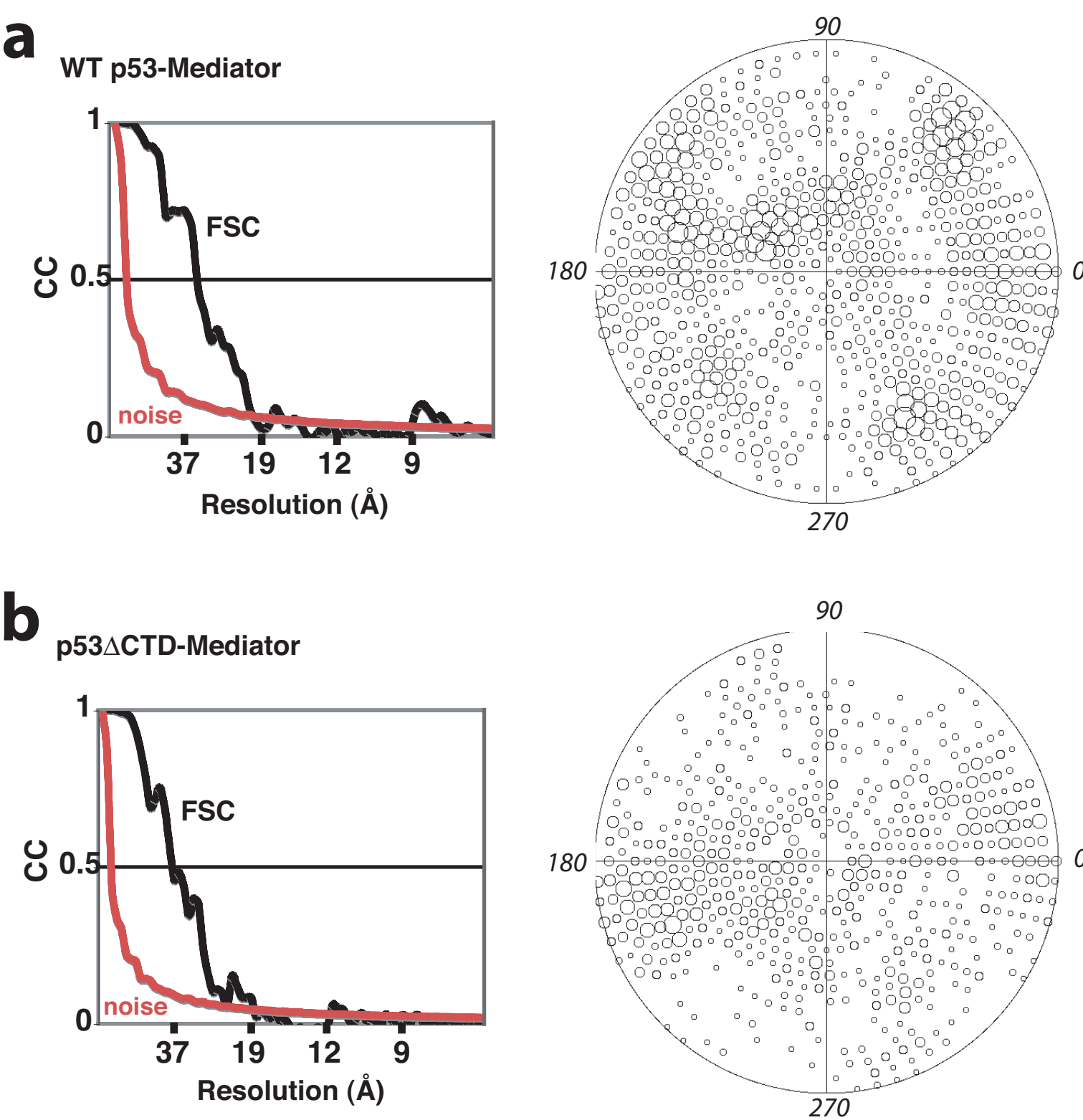

Supplementary Figure 12 | Image processing data from 3D reconstruction of WT p53-Mediator **(a)** and p53ΔCTD-Mediator **(b)**. Single-particle angular distribution for each data set is shown, along with the Fourier Shell Correlation coefficient (FSC) and 3σ noise plots vs. spatial resolution.

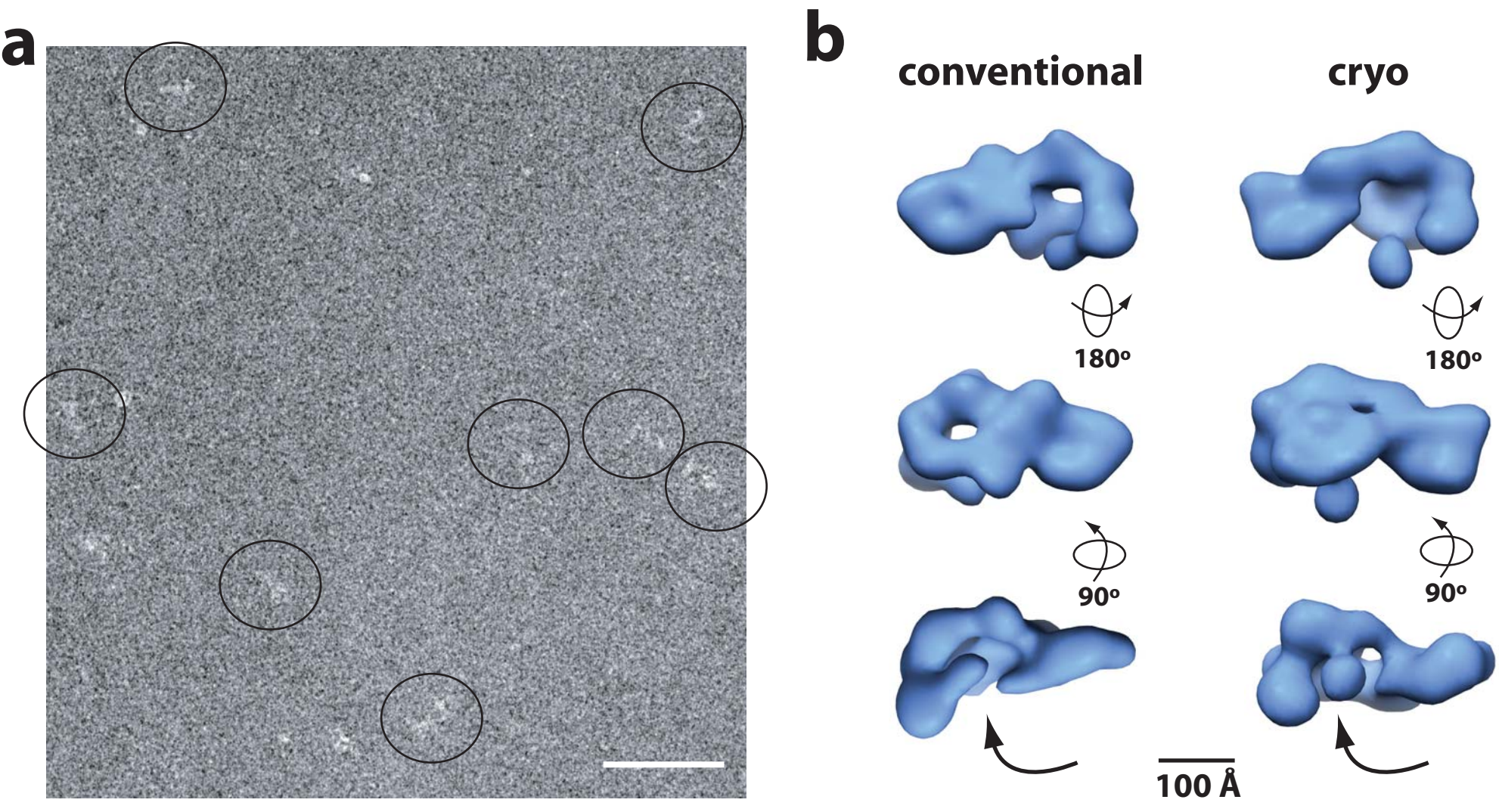

Supplementary Figure 13 | Cryo-EM analysis of p53AD–Mediator. (a) Micrograph of cryo-negatively-stained p53AD–Mediator sample. p53AD–Mediator complexes are circled; image is contrast-enhanced to facilitate visualization. Bar: 100 nm. **(b)** Comparison of conventional negative-stain p53AD–Mediator reconstruction (also shown in **Fig. 5a**) with the cryo-EM reconstruction, which used data from a frozen-hydrated p53AD–Mediator sample. Similar views of each structure are shown, and each is rendered to 1.2 MDa. The pocket domain is highlighted with an arrow.

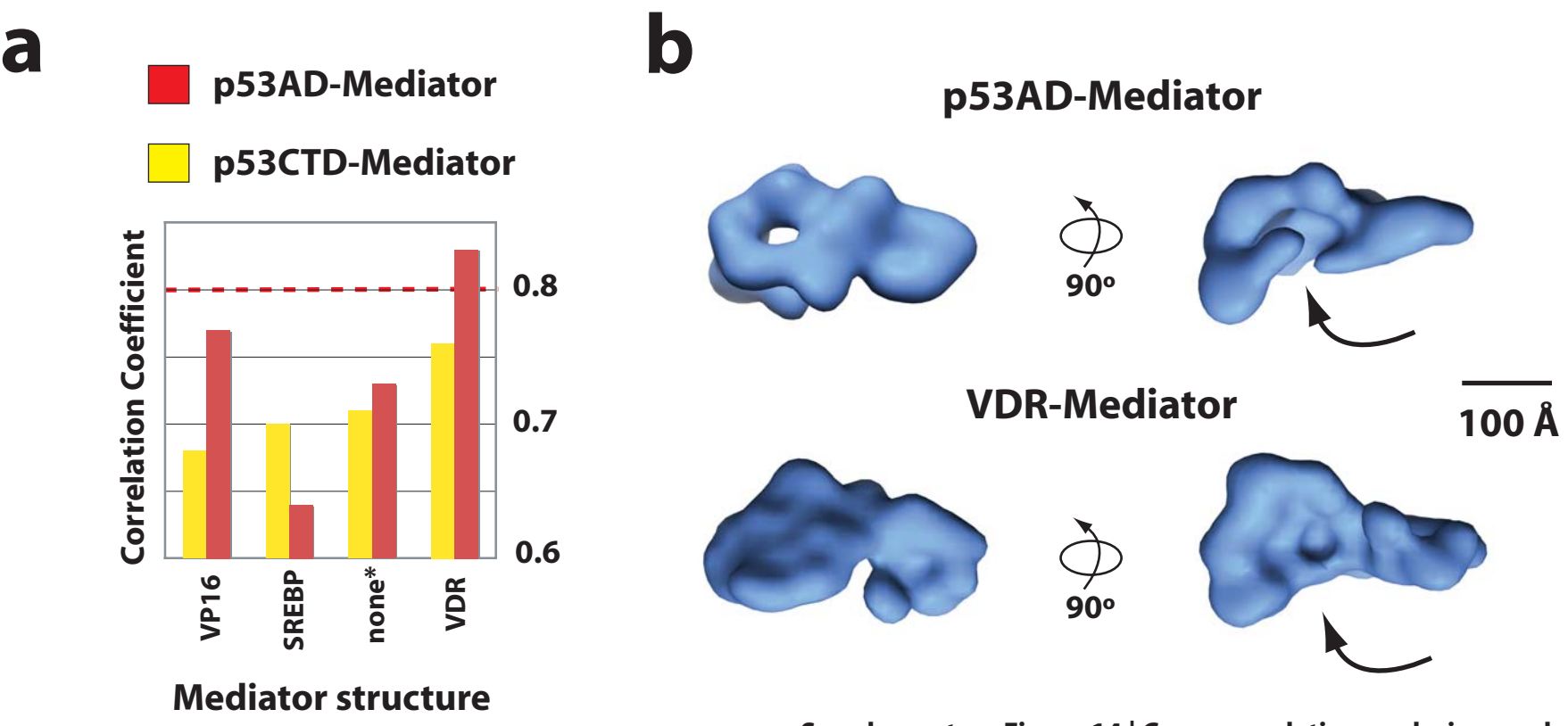

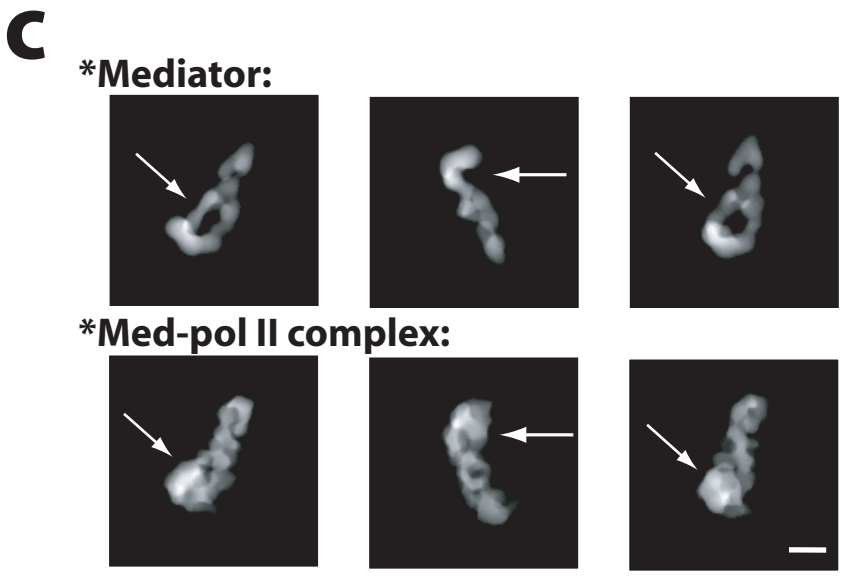

Supplementary Figure 14 | Cross-correlation analysis reveals p53AD-Mediator resembles other activator-bound Mediator structures whereas p53CTD–Mediator is structurally distinct. (a) Bar graph showing cross-correlation coefficients for different Mediator structures relative to p53AD-Mediator (red bars) or p53CTD–Mediator (yellow bars). Correlation values were calculated with Chimera[25]. Note that *none represents the unliganded Mediator structure, which is not bound to an activator, whereas VP16, SREBP, and VDR represent Mediator structures bound to VP16, SREBP, and VDR[11,13]. A cross-correlation value of 0.80 or greater is indicative of conformational similarity, as described elsewhere[13]. **(b)** VDR and p53AD induce similar structural shifts upon binding Mediator. Direct comparison of the EM structures of p53AD–Mediator and VDR–Mediator[13]. Similar views are shown and the pocket domain in each structure is noted with an arrow. Each complex is rendered to 1.2 MDa. **(c) Human RNA polymerase II binds Mediator at the pocket domain.** Noise-free 2D projections are shown of Mediator only (top) or a Mediator-pol II complex (bottom). Arrows highlight the pocket domain (top panels) and indicate this region becomes occupied upon addition of pol II (bottom panels). *Note that for these experiments, Mediator was bound to VP16[11]. Bar: 100 Å.

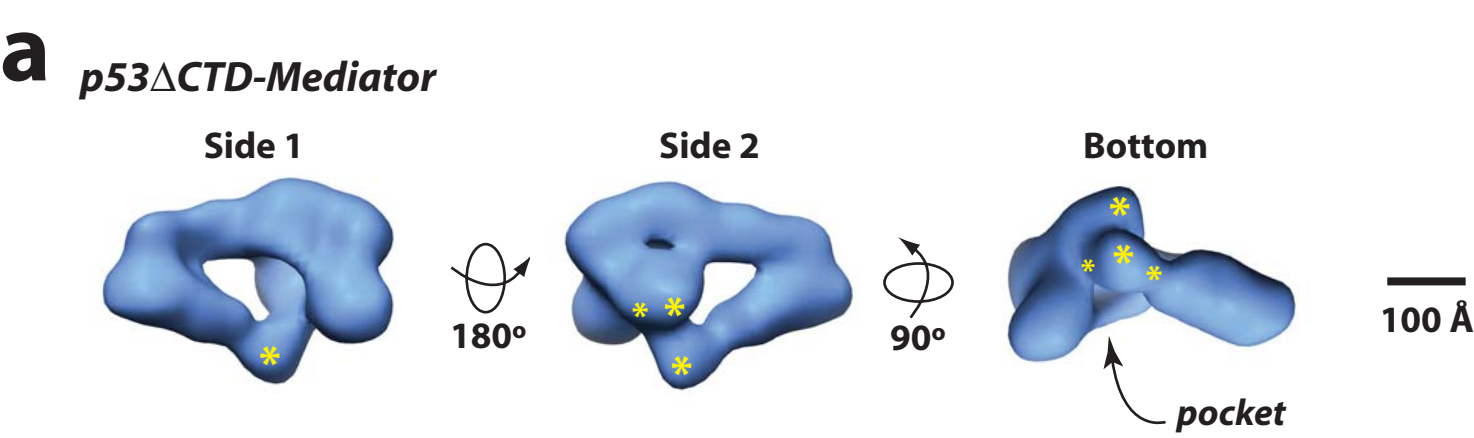

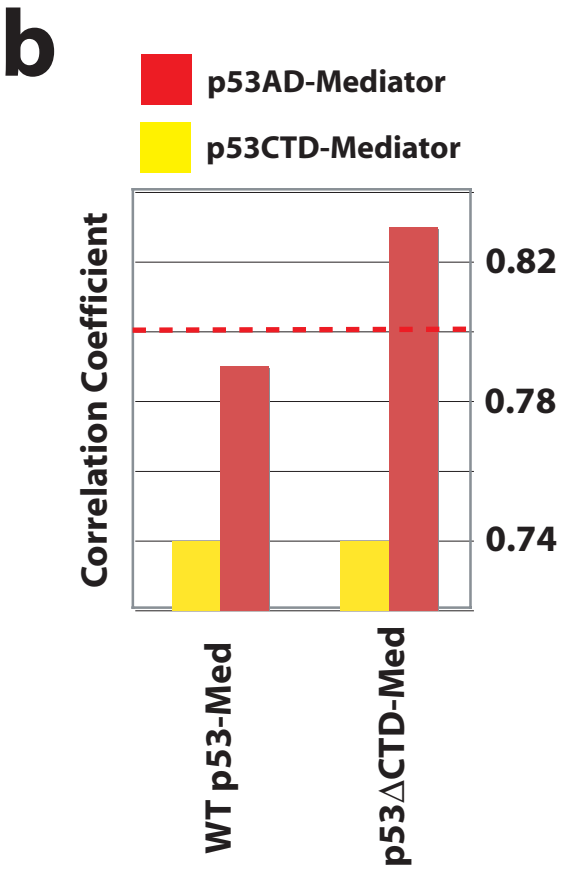

Supplementary Figure 15 | Structure of p53ΔCTD–Mediator and cross-correlation analysis. (a) Three different views of the structure of Mediator bound to p53 tetramers lacking the p53CTD (residues 1-362: p53ΔCTD). Volume was resolved to 36 Å resolution and rendered to 1.4 MDa, consistent with the approximate molecular weight of the complex. A defined pocket domain is evident in the structure, similar to that observed with WT p53–Mediator (**Fig. 5c**). The general location of the p53 tetramer was determined by docking the WT p53 tetramer into the p53ΔCTD–Mediator structure using SITUS[38]; asterisks represent the p53 DNA-binding domains. Larger asterisks are closer to the viewer. Bar: 100 Å. **(b)** Bar graph showing cross-correlation coefficients for p53 tetramer-bound Mediator structures relative to p53AD–Mediator (red bars) or p53CTD–Mediator (yellow bars). Correlation values were calculated with Chimera[25]. Note that WT p53 and p53ΔCTD denote p53 tetramer–Mediator structures shown in **Figure 5c** and part **a**, above. A cross-correlation value of 0.80 or greater is indicative of conformational similarity, as described[13].

SUPPLEMENTARY INFORMATION

Terminology: Pre-Elongation Complex and stalled pol II

The term Pre-Initiation Complex (PIC) has been used to describe the entire transcriptional apparatus, which includes TFIIA, IIB, IID, IIE, IIF, IIH, Mediator, and pol II[1]. Appropriately, PIC indicates that transcription initiation, by any measure, has not yet occurred. In light of recent observations that a significant fraction of metazoan genes harbor stalled pol II complexes—that is, polymerases that have initiated transcription but have not transitioned to a productively-elongating state—we propose the term Pre-Elongation Complex (PEC). Unlike the term PIC, PEC more broadly defines the initiation machinery and implies only that pol II has not transitioned to a productively-elongating state. Thus, PEC is a more generic descriptor that encompasses a range of functional states, including stalled, promoter-bound pol II complexes. In this manuscript, we will use PEC instead of PIC when referring to the transcription initiation machinery (i.e. TFIIA, IIB, IID, IIE, IIF, IIH, Mediator, and pol II). One caveat, however, is that it is not clear whether all PEC components are similarly present at promoters that contain stalled polymerases (e.g. does TFIIB remain associated in this context?) versus those that do not.

With respect to the terminology used to describe promoter-bound pol II, there is no consensus about what term (e.g. paused, stalled, poised, pre-loaded, arrested) to use to describe a promoter-associated pol II complex that is not actively transcribing. One reason for this is that at any given gene, promoter-associated polymerases that are not actively transcribing represent a mixed population of states[2]. Some appear to be truly "paused," that is, they will at some point become activated and transition to a productively-elongating state. However, a population of polymerases also appear to be "arrested," that is, they will not make this transition[3]. Given that such inactive, promoter-bound polymerases appear to represent a mixed population of states (some will ultimately transcribe, and others will never transcribe), we adopted the term "stalled" because it implies that both possibilities can occur. This term has been used in the past to describe pol II complexes that are promoter-associated but not actively transcribing[4,5].

SUPPLEMENTARY RESULTS AND DISCUSSION

The p53CTD represents the second p53 domain that interacts with Mediator

The p53CTD (residues 363-393) interacts with Med1. Past studies have shown that p53 interacts with Mediator through two different subunits: Med17 and Med1[6,7]. Although p53AD was known to bind Med17, the p53 domain responsible for interaction with Med1 was not known. Yet this second, Med1-interacting domain within p53 was shown to reside outside the p53AD, based upon in vitro binding assays with p53AD mutants[7]. To identify the p53 domain responsible for interaction with the Med1 subunit of Mediator, we generated p53 constructs that contained residues 293-393, 293-363, or 363-393. These three p53 domains comprise regions outside its DNA-binding domain (which would be unlikely to mediate direct interactions with Med1) and are not within p53AD. Residues 363-393 were tested specifically on the basis that these residues are accessible and disordered within the native p53 tetramer structure[8]. As shown in **Supplementary Figure 1a**, in vitro transcription/translation experiments revealed that GST fusion proteins containing residues 363-393 were capable of binding [^{35}S]-labeled Med1 (lanes 3 and 5), whereas the p53 construct lacking this domain could not bind Med1 (residues 293-363, lane 4). Similarly, p53 residues 293-363 could not pull down Mediator from crude extracts, whereas Mediator was retained on a p53 (363-393) affinity resin (**Supplementary Fig. 1b**).

Next, we tested whether p53 residues 363-393 (hereafter called p53CTD) would be capable of purifying Mediator from partially-purified extracts (the P1.0M/Q1.0M fraction) enriched in Mediator. After binding, the GST-p53CTD resin was washed extensively with 0.5M KCl HEGN and eluted. The silver-stained gel shown in **Supplementary Figure 1c** reveals a pattern of bands characteristic of Mediator, and the identity of numerous polypeptides in this sample was confirmed by western blotting (**Supplementary Fig. 1d**). Based upon the data in **Supplementary Figure 1**, it appeared the p53CTD defined the second p53 domain previously observed to interact with Mediator through Med1[6,9]. To further confirm the p53CTD–Mediator interaction, we performed additional structural and functional assays, described below.

Mediator affinity purified with p53AD or p53CTD possesses the same potential activity. Although the data in **Supplementary Figure 1** indicated the p53CTD was capable of binding Mediator, it remained possible the Mediator polypeptide composition might be different when purified with the p53CTD affinity resin. Potential subunit differences might result in alterations in Mediator co-activator function. To compare the activity of Mediator purified with p53AD versus p53CTD, we utilized a reconstituted transcription system[10]. Because the reconstituted assay requires Mediator for transcription activation, it provided a reliable means to assess the co-activator function of each independently-purified Mediator sample. Therefore, Mediator—purified with either a p53AD or p53CTD affinity resin—was titrated into transcription reactions as shown in **Supplementary Figure 1e**. The data reveal that Mediator co-activator function was equivalent for each sample: Mediator purified with a p53AD or p53CTD affinity resin each potentiated activator-dependent transcription in a dose-dependent manner (**Supplementary Fig. 1e**; compare lanes 2-4 and 6-8). These results demonstrate that the Mediator complex isolated via the p53CTD alone was functionally indistinguishable from Mediator purified by alternate means (e.g. with a p53AD affinity resin). Note, however, that this experiment does not address whether potential structural changes might impact Mediator co-activator function since transcription in **Supplementary Figure 1e** is driven by promoter-bound Sp1, not p53.

Binding of p53CTD to unliganded Mediator induces the predicted structural shift. Because of the unique structural features observed with p53CTD–Mediator (**Fig. 5b** and **Supplementary Fig. 14a**), we sought to confirm that these structural shifts were in fact induced by p53CTD binding and did not simply represent potential differences in subunit composition. Therefore, we isolated an unliganded (activator-free) Mediator sample whose subunit composition and structure has been determined previously[11]. Then, p53CTD was added to this unliganded Mediator sample. After 1h incubation, this sample was analyzed using EM (**Supplementary Fig. 2a**) and an independent, 3D reconstruction was completed to establish whether the predicted structural shifts occurred within the complex. Importantly, this independent 3D reconstruction was conducted using random conical tilt methods and therefore was completed without reference bias. A comparison of the "converted" p53CTD–Mediator structure with the conventionally-purified sample is shown in **Supplementary Figure 2b**. Although the converted structure was not 100% identical to the conventionally-purified complex, its molecular architecture clearly represents the p53CTD–Mediator conformational state.

Mediator is not a static, conformationally rigid complex. Rather, Mediator is quite dynamic, capable of stably adopting different structural states and maintaining a degree of flexibility within each. Although p53 binding clearly stabilizes one particular conformational state over the others, it is clear that the 3D structures resolved by EM represent an average conformation about which the structure oscillates. Thus, independent 3D reconstructions from different p53CTD–Mediator samples yield complexes that clearly represent the same conformational state, yet do not have 100% identical structures. Structural differences between the converted and conventional p53CTD–Mediator structures were not unexpected, based upon the fact that 1) the converted structure sample was isolated using a completely different protocol; 2) a significant portion of Mediator complexes in the conversion experiment likely represent unliganded Mediator itself. Although this heterogeneity can be mitigated through 2D classification and cross-correlation, unliganded Mediator likely contributes to variation within the converted structure: not all unliganded Mediator complexes will be bound to p53CTD. This is also reflected in the across-the-board lower cross-correlation coefficients observed upon comparison of converted p53CTD–Mediator with other Mediator structures (**Supplementary Fig. 2c**); and 3) the 3D reconstruction of the converted p53CTD–Mediator was completed independent of any reference structure, using random-conical tilt methodology[12]. Past conversion experiments with VP16, SREBP, and VDR yielded similar results in which the converted structures were similar, but not identical, to the conventionally purified samples[11,13].

Importantly, the converted p53CTD–Mediator structure contains features that closely resemble the structure determined by conventional means (**Supplementary Fig. 2b**), including the V-shaped density along Side 1 and the wall of density at the pol II binding site. Structural conversion by p53CTD was also

borne out by the cross-correlation data (**Supplementary Fig. 2c**), which indicate that the converted p53CTD–Mediator structure correlates most highly with the p53CTD–Mediator structure isolated by conventional means. By contrast, lower cross-correlation coefficients were calculated upon comparison of the converted p53CTD–Mediator structure with SREBP–Mediator, VP16–Mediator, p53AD–Mediator, or unliganded Mediator, as expected (**Supplementary Fig. 2c**). The structural comparison outlined in **Supplementary Figure 2** confirms that the unique structural features observed within p53CTD–Mediator are a direct consequence of p53CTD binding and do not result from major differences in subunit composition, since the initial unliganded Mediator sample used for the p53CTD structural conversion experiment has a defined, consensus Mediator subunit composition[11]. Further evidence for p53CTD-directed structural shifts within Mediator was obtained upon analysis of Mediator bound to wild-type and mutant p53 tetramers (see **Fig. 5c** and **Supplementary Fig. 15**).

NELF occupancy at HDM2 and p21

The multi-subunit NELF complex has been shown to regulate transcription initiation and appears to operate in part by controlling the transition of promoter-bound pol II to a productively-elongating state[14]. A previous study that examined estrogen receptor (ER) target genes revealed that promoter-bound NELF correlated with genes that contained pre-loaded pol II; however, NELF occupancy at these genes did not significantly change upon gene activation[15]. We observed similar results at the *HDM2* and *p21* genes. ChIP assays revealed that NELF occupied the promoter region of *HDM2* and *p21* before induction, and NELF occupancy did not change upon activation by WT p53 or p53ΔCTD (**Supplementary Fig. 9**). A decrease in NELF occupancy was observed in the presence of the transcriptionally inactive p53QS mutant, hinting that NELF might act to positively regulate *HDM2* and *p21* expression, as observed for a subset of genes in *Drosophila*[16]. However, the NELF complex was not included in our reconstituted transcription assays and the major, p53AD-dependent differences in mRNA levels measured in cells (**Fig. 3c, d**) were recapitulated in our reconstituted transcription assays (**Fig. 2c** and **Fig. 3a**). Consequently, although NELF may play auxiliary roles in regulating *HDM2* and *p21* expression, it does not appear to be the major factor that controls p53AD-dependent changes in PEC/pol II activation.

The structural state of Mediator is controlled by p53AD and p53CTD

Mediator purification with a p53AD affinity resin. Given previous results that indicated a direct interaction between p53AD (residues 1-73) and the Med17 subunit of Mediator[7], we tested whether p53AD would bind the entire Mediator complex with sufficient affinity and specificity to enable purification of Mediator from a partially-purified extract. Other activation domains, including VP16 and SREBP-1a, could reliably isolate Mediator when immobilized onto a resin[17]. Therefore, we prepared a p53AD affinity resin and incubated it together with the P1M/Q1M fraction, which is derived from HeLa nuclear extract and is enriched in Mediator and other general transcription factors, including TFIID, TFIIH, and pol II (**Supplementary Fig. 10a**). Like other transcription factor activation domains, p53AD specifically bound Mediator and provided a reliable means to purify the complex from the P1M/Q1M fraction (**Supplementary Fig. 10b, c**). As anticipated[7,18], introduction of oncogenic L22Q, W23S mutations within the p53AD affinity resin (residues 1-73) abolished its ability to purify Mediator (data not shown).

Cryo-EM analysis of p53AD–Mediator. For each of the EM structures shown in **Figure 5**, data was collected from samples negatively-stained with 4% uranyl acetate in water. Prior to application of this solution, we completed buffer exchange on the grid with a solution containing 5% trehalose. The inclusion of trehalose increases the hydration of the negatively-stained samples and minimizes the likelihood of flattening[19-21]. Indeed, Mediator samples prepared in this way do not show significant flattening; evidence of flattening would be detected upon screening and cross-correlation of data collected using random conical tilt[22-24].

However, to further ensure the integrity of our 3D reconstructions of p53–Mediator, and to confirm that significant flattening was not occurring in the negatively-stained samples, we analyzed p53AD–Mediator in its fully hydrated state using vitrified (cryo-EM) samples (**Supplementary Fig. 13a**). Shown in

Supplementary Figure 13b is a comparison of the 3D structures of p53AD–Mediator obtained from conventional or cryo-EM data. Major structural features are preserved in each structure, and this is reflected in the high cross-correlation coefficient (0.81) between the structures. The prominent pocket domain (arrow in **Supplementary Fig. 13b**) is also evident in each reconstruction, and the dimensions (length, width, height) are similar for both the cryo and conventional EM 3D volumes. Thus, as expected, the data in **Supplementary Figure 13** indicate no significant differences in the p53AD–Mediator structure when evaluated with frozen-hydrated samples.

p53AD–Mediator resembles other activator-bound Mediator structures whereas p53CTD–Mediator is structurally distinct. To evaluate the structural similarities and differences between p53AD- and p53CTD–Mediator relative to other Mediator structural states, we completed cross-correlation analysis of p53-bound Mediator structures using Chimera[25]. Cross-correlation values were calculated and are plotted in **Supplementary Figure 14a**, with red bars representing cross-correlation coefficients for p53AD–Mediator versus different previously-published Mediator structures listed along the x-axis. Cross-correlation coefficients for p53CTD–Mediator are shown with yellow bars in **Supplementary Figure 14a**. Note that conformational similarity is represented by correlation values of 0.80 or greater, as described elsewhere[13].

Interestingly, the p53AD–Mediator structure correlates well with VDR–Mediator (CC = 0.83). Similar views of these Mediator structures are shown in **Supplementary Figure 14b**, with the pocket domain in each denoted by an arrow. In contrast, the p53CTD–Mediator structure does not correlate well with other Mediator structures: in no instance does its cross-correlation value match or exceed 0.80. The activity of p53CTD–Mediator is also distinct in that it is unable to support activated transcription (see **Fig. 2c**, lane 5). Thus, p53CTD–Mediator represents a complex that is structurally and functionally distinct from other activator-bound Mediator structures.

EM analysis of Mediator bound to wild-type and mutant p53 tetramers. We next examined whether structural features within p53AD–Mediator—specifically the pol II pocket domain—would be preserved upon p53 tetramer binding to Mediator. As shown in **Figure 5c**, the pocket domain was preserved within the structure of Mediator bound to wild-type p53 tetramers (see also **Supplementary Movie 3**). We also examined Mediator structure bound to the p53ΔCTD tetramer, which, like WT p53, is able to activate transcription in vitro (**Fig. 3a**, lane 6) and in cells (**Fig. 3c, d**). p53ΔCTD tetramers (aa 1-362) contain the activation domain but lack the 31-residue p53CTD. Similar to WT p53–Mediator, the p53ΔCTD–Mediator structure also possesses a prominent pocket domain (**Supplementary Fig. 15a** and **Supplementary Movie 4**), further highlighting the link between Mediator structure and its co-activator function. In particular, the p53AD→Med17 interaction appears to control formation of the pocket domain, which correlates with activation of pre-loaded, promoter-bound pol II.

Docking the p53 tetramer structure within WT p53–Mediator. To assess the location of the p53 tetramer within the WT p53–Mediator structure, we used SITUS and Chimera to dock the structure of the p53 tetramer[8] into the WT p53–Mediator EM map. Similar docking results were obtained with SITUS and Chimera. In **Figure 5c**, the location of the p53 tetramer is denoted by asterisks, which represent the DNA-binding domains within the tetramer. An overlay showing the docked p53 tetramer within the EM map of WT p53–Mediator is also shown in **Figure 5c**. p53 tetramer docking could clearly localize the four DNA-binding domains, whereas 2 of 4 of the p53AD/CTD nodes appeared to be shifted considerably. This was anticipated based upon the fact that p53AD and p53CTD each interact with Mediator directly, and their interaction with Mediator likely requires dissociation of the p53AD-p53CTD node within the p53 tetramer structure[8]. Although the docking experiment clearly localizes the p53 tetramer within the WT p53–Mediator structure, a more precise localization of the DNA binding domains and other p53 domains (e.g. the oligomerization domain or p53AD) awaits further structural analysis with frozen-hydrated WT p53–Mediator samples.

Both p53AD and p53CTD direct structural shifts upon p53 tetramer-Mediator binding. By evaluating WT p53- and p53ΔCTD–Mediator by cross-correlation against p53AD- and p53CTD–Mediator, we could examine whether p53AD and p53CTD might work together to direct structural changes in Mediator. As shown in **Supplementary Figure 15b**, this analysis revealed that when bound to the wild-type p53 tetramer, Mediator does not adopt a structural state that correlates highly with Mediator bound to p53AD or p53CTD alone. This suggests that p53AD and p53CTD coordinately control Mediator structure upon tetramer binding. Indeed, if only p53AD-directed structural shifts were important in the context of the p53 tetramer, the structural state of WT p53–Mediator should have correlated highly (> 0.80) with p53AD–Mediator, but this was not observed. Rather, WT p53–Mediator adopts a structure distinct from p53AD–Mediator, based upon cross-correlation analysis.

To further evaluate whether the p53CTD was in fact contributing to Mediator structural shifts upon p53 tetramer binding, we performed an independent EM analysis (using random conical tilt methods) of Mediator bound to the p53ΔCTD tetramer. These mutant p53 tetramers contain the activation domain but lack the p53CTD. Thus, if the p53CTD was directing structural shifts upon WT p53 binding, the structure of p53ΔCTD–Mediator should more closely resemble the Mediator structure bound to p53AD alone (i.e. p53AD–Mediator). As predicted, this was in fact observed: the p53AD–Mediator structure correlates highly (CC = 0.83) with the p53ΔCTD–Mediator structure but not the WT p53–Mediator structure (**Supplementary Fig. 15b**). That independent 3D reconstructions of WT p53–Mediator and p53ΔCTD–Mediator each correlate exactly as predicted (e.g. p53ΔCTD–Mediator correlates highly with p53AD–Mediator) reflects the integrity of the structural data and strongly supports our interpretation of these data. Taken together, the data in **Supplementary Figure 15** indicate the p53CTD contributes to the structural shifts within WT p53–Mediator and that p53AD and p53CTD coordinately control Mediator structure upon p53 tetramer binding.

Given the direct link between Mediator structure and its co-activator function, as described here, what are the functional consequences of the p53CTD-directed structural shifts? Further work will be necessary to evaluate the potential impact of the p53CTD on Mediator function. The p53CTD is important to properly regulate the p53 transcriptional response. In fact, p53 target gene expression patterns are disrupted in p53CTD mutants[26-30] and the p53CTD appears to play many roles in p53 function, including regulation of p53 stability, DNA binding, and co-activator recruitment[31-35]. The structural studies described here suggest an additional regulatory role for the p53CTD might involve structural shifts within Mediator that may serve important regulatory functions at a subset of p53 target genes.

EM analysis of the Mediator-pol II complex

To isolate the Mediator-pol II assembly, each complex was purified as described[10] and incubated together for 1h at 4ºC. After incubation, the sample was run over a glycerol gradient to separate Mediator-pol II complexes from the free, unbound pol II enzyme. Samples containing pol II-Mediator were then imaged in negative stain using EM and random conical tilt methods. The data derived from analysis of negatively-stained samples of Mediator-pol II (**Supplementary Fig. 14c**) clearly shows that pol II occupies the pocket domain within Mediator. Shown in **Supplementary Figure 14c** are noise-free, two-dimensional projections (generated from 3D volumes) of either Mediator alone (bound to VP16) or the Mediator-pol II complex. The VP16–Mediator structure has been published[11], whereas a more detailed structural analysis of the Mediator-pol II complex will be provided elsewhere (C. Bernecky and D. Taatjes, unpublished results). The data shown here simply confirm that pol II binds at the pocket site within human Mediator, in agreement with past structural studies with yeast Mediator[36].

SUPPLEMENTARY METHODS

Recombinant proteins. p53AD: residues 1-73, p53CTD: residues 363-393, p53AD/CTD: residues 1-73/323-393. For Mediator purification, these domains were cloned into the pGEX-4T-3 vector, expressed in *E. coli* and purified with a glutathione-sepharose resin (GE Healthcare). For in vitro transcription assays, each p53 domain was sub-cloned to the GAL4 DNA-binding domain (aa 1-94). Full-length (1-1581), GST-

tagged human Med1 was expressed in baculovirus-infected Sf9 cells. Full-length (1-651), GST-tagged Med17 was expressed in *E. coli*.

Immobilized template assays. A biotinylated GAL4 promoter construct (containing 5 GAL4 binding sites upstream of TATA box) was immobilized onto NeutrAvidin beads (Pierce), essentially as described[39]. Activators (2 nM GAL4-p53AD/CTD or GAL4-p53CTD) were incubated with 50 ng immobilized template in binding buffer (0.11M KCl, 12.5mM HEPES pH 7.9, 62.5 μM EDTA, 63 μM $ZnCl_2$, 50 mg/ml BSA, 12.5% glycerol, 0.025% NP-40) in the presence of HeLa nuclear extract (350 μg total protein) at 25°C for 45 minutes. Immobilized templates were then washed five times with 100 column volumes wash buffer (same as binding buffer except 0.2M KCl and no BSA). Bound proteins were eluted with SDS loading buffer and filtered (0.4 μm) prior to analysis. Note that control experiments without an activator revealed full PEC occupancy (data not shown), in agreement with past studies using immobilized templates with human or yeast cell extracts[40,41]. In these experiments, PEC assembly was clearly driven by the core promoter, as mutation of the TATA box was required to block PEC assembly[39-41].

Chromatin sedimentation. Chromatin sedimentation was completed following PEC assembly with purified components in vitro, as described[10].

p53-Med1 binding assays. A fragment of Med1 (residues 1234-1406) previously shown to interact with p53[6] was expressed and [^{35}S]-labeled using a rabbit reticulocyte lysate, according to standard protocol (Promega). This lysate was then incubated over resin bound to p53 residues 293-393, 293-363, or 363-393. Following a series of washes with 0.5M KCl HEGN (5 x 20 column volumes) and 0.15M KCl HEGN (1 x 20 column volumes), bound material was eluted with 30 mM glutathione buffer and separated by gel electrophoresis. The ^{35}S-labeled Med1 was visualized by autoradiography.

Reporter assays. GAL4-p53AD or GAL4-p53CTD was transfected into HEK-293 cells along with a luciferase reporter vector containing GAL4 binding sites. Luminescence was measured from extracts prepared from either population of cells and compared to a renilla standard according to manufacturers protocol (Promega). Data reported is from 3 separate transfection experiments, each performed in triplicate.

Immobilized template kinase assays. Activators (10 nM final concentration; WT p53 or p53QS) were added to immobilized HDM2 template DNA (180 ng). After 30 minutes incubation at 27 ºC, PEC components (30 nM TFIIA, 10 nM TFIIB, 1 nM TFIID, 10 nM TFIIE, 10 nM TFIIF, 1 nM TFIIH, 2 nM pol II, 5 nM Mediator) were added. Fifteen minutes was allowed for PEC assembly at 27 ºC. To remove unbound factors, immobilized templates were then washed with 10 column volumes of transcription buffer (10 mM HEPES pH 7.6, 60 mM KCl, 7% glycerol, 6 mM $MgCl_2$, 0.1 mM EDTA, 0.1 mM EGTA, 0.5% PEG, 0.5% polyvinyl alcohol), followed by the addition of NTPs (to 1 mM each, including [^{32}P]-ATP). Reactions were stopped by adding SDS loading buffer; the samples were then immediately frozen in liquid nitrogen until analysis.

EM analysis of Mediator-pol II complex. EM analysis of Mediator-pol II complexes was completed as described for p53–Mediator complexes, except that individual images were windowed into 161x161 pixel boxes. Note that Mediator was purified bound to VP16 for the Mediator-pol II structural analysis. Following 2D classification of single-particle images and cross-correlation to establish a homogenous data set, a 3D reference volume (obtained from 6430 single-particle images) of the Mediator-pol II complex was subjected to angular refinement as described[13]. The Mediator-pol II complex was filtered to 37 Å resolution, based upon the 0.5 Fourier shell correlation criterion[42]. A structure of VP16–Mediator alone[11] was similarly filtered to 37 Å resolution and aligned to the Mediator-pol II complex. One hundred ninety-four noise-free 2D projections (corresponding to a 10º angular step) were then generated from each aligned 3D reconstruction (VP16–Mediator or VP16–Mediator-pol II); three projection views that best highlight the pol II density are shown in **Supplementary Figure 14c**.

Cross-correlation analysis. Alignment and cross-correlation of 3D reconstructions were completed with Chimera, using the "fit map-in-map" function. Alignments were also completed using SITUS and yielded identical results.

SUPPLEMENTARY REFERENCES

1. Hahn, S. Structure and mechanism of the RNA polymerase II transcription machinery. *Nat Struct Mol Biol* **11**, 394-403 (2004).
2. Gilmour, D.S. Promoter proximal pausing on genes in metazoans. *Chromosoma* **118**, 1-10 (2009).
3. Rasmussen, E.B. & Lis, J.T. Short transcripts of the ternary complex provide insight into RNA polymerase II elongational pausing. *J Mol Biol.* **252**, 522-535 (1995).
4. Muse, G.W. et al. RNA polymerase is poised for activation across the genome. *Nat Genet.* **39**, 1507-1511 (2007).
5. Zeitlinger, J. et al. RNA polymerase stalling at developmental control genes in the Drosophila melanogaster embryo. *Nat Genet.* **39**, 1512-1516 (2007).
6. Drane, P., Barel, M., Balbo, M. & Frade, R. Identification of RB18A, a 205 kDa new p53 regulatory protein which shares antigenic and functional properties with p53. *Oncogene* **15**, 3013-24 (1997).
7. Ito, M. et al. Identity between TRAP and SMCC complexes indicates novel pathways for the function of nuclear receptors and diverse mammalian activators. *Mol. Cell* **3**, 361-370 (1999).
8. Okorokov, A.L. et al. The structure of p53 tumor suppressor protein reveals the basis for its functional plasticity. *EMBO J* **25**, 5191-5200 (2006).
9. Frade, R., Balbo, M. & Barel, M. RB18A, whose gene is localized on chromosome 17q12-q21.1, regulates in vivo p53 transactivating activity. *Cancer Research* **60**, 6585-6589 (2000).
10. Knuesel, M.T., Meyer, K.D., Bernecky, C. & Taatjes, D.J. The human CDK8 subcomplex is a molecular switch that controls Mediator co-activator function. *Genes & Development* **23**, 439-451 (2009).
11. Taatjes, D.J., Naar, A.M., Andel, F., Nogales, E. & Tjian, R. Structure, Function, and Activator-Induced Conformations of the CRSP Coactivator. *Science* **295**, 1058-1062 (2002).
12. Radermacher, M., Wagenknecht, T., Verschoor, A. & Frank, J. Three-dimensional reconstruction from a single-exposure random conical tilt series applied to the 50s ribosomal subunit of Escherichia coli. *J. Microsc.* **146**, 113-136 (1987).
13. Taatjes, D.J., Schneider-Poetsch, T. & Tjian, R. Distinct conformational states of nuclear receptor-bound CRSP-Med complexes. *Nat Struct Mol Biol* **11**, 664-671 (2004).
14. Saunders, A., Core, L.J. & Lis, J.T. Breaking barriers to transcription elongation. *Nat Rev Mol Cell Biol* **7**, 557-567 (2006).
15. Kininis, M., Isaacs, G.D., Core, L.J., Hah, N. & Kraus, W.L. Postrecruitment regulation of RNA polymerase II directs rapid signaling responses at the promoters of estrogen target genes. *Mol Cell Biol* **29**, 1123-1133 (2009).
16. Gilchrist, D.A. et al. NELF-mediated stalling of pol II can enhance gene expression by blocking promoter-proximal nucleosome assembly. *Genes & Development* **22**, 1921-1933 (2008).
17. Naar, A.M. et al. Composite co-activator ARC mediates chromatin-directed transcriptional activation. *Nature* **398**, 828-832 (1999).
18. Lin, J., Chen, J., Elenbaas, B. & Levine, A.J. Several hydrophobic amino acids in the p53 amino-terminal domain are required for transcriptional activation, binding to mdm-2 and the adenovirus 5 E1B 55-kD protein. *Genes & Development* **8**, 1235-1246 (1994).
19. Green, J.L. & Angell, C.A. Phase relations and vitrification in saccharide-water solutions and the trehalose anomaly. *J. Phys. Chem.* **93**, 2880-2882 (1989).
20. Harris, J.R. & Scheffler, D. Routine preparation of air-dried negatively stained and unstained specimens on holey carbon support films: a review of applications. *Micron* **33**, 461-480 (2002).
21. Ohi, M., Li, Y., Cheng, Y. & Walz, T. Negative staining and image classification--powerful tools in modern electron microscopy. *Biol. Proced. Online* **6**, 23-34 (2004).

22. Cheng, Y. et al. Single particle reconstructions of the transferrin-transferrin receptor complex obtained with different specimen preparation techniques. *J. Mol. Biol.* **355**, 1048-1065 (2006).
23. Leschziner, A.E. & Nogales, E. The orthogonal tilt reconstruction method: an approach to generating single-class volumes with no missing cone for ab initio reconstruction of asymmetric particles. *J. Struct. Biol.* **153**, 284-299 (2006).
24. Radermacher, M. & Ruiz, T. Three-dimensional reconstruction of single particles in electron microscopy. in *Methods in Molecular Biology*, Vol. 319 (eds. Taatjes, D.J. & Mossman, B.T.) 427-461 (Humana Press, Totowa, NJ, 2006).
25. Pettersen, E.F. et al. UCSF Chimera--A visualization system for exploratory research and analysis. *J Comput. Chem.* **25**, 1605-1612 (2004).
26. Bourdon, J. et al. p53 isoforms can regulate p53 transcriptional activity. *Genes & Development* **19**, 2122-2137 (2005).
27. Almog, N., Goldfinger, N. & Rotter, V. p53-dependent apoptosis is regulated by a C-terminally alternatively spliced form of murine p53. *Oncogene* **19**, 3395-3403 (2000).
28. Goldschneider, D. et al. Expression of C-terminal deleted p53 isoforms in neuroblastoma. *Nucleic Acids Research* **34**, 5603-5612 (2006).
29. Wu, Y., Liu, Y., Lee, L., Miner, Z. & Kulesz-Martin, M. Wild-type alternatively spliced p53: binding to DNA and interaction with the major p53 protein in vitro and in cells. *EMBO J* **13**, 4823-4830 (1994).
30. Zhou, X. et al. COOH-terminal domain of p53 modulates p53-mediated transcriptional transactivation, cell growth, and apoptosis. *Cancer Research* **59**, 843-848 (1999).
31. McKinney, K., Mattia, M., Gottifredi, V. & Prives, C. p53 linear diffusion along DNA requires its C terminus. *Mol Cell* **16**, 413-424 (2004).
32. Gu, W. & Roeder, R.G. Activation of p53 sequence-specific DNA binding by acetylation of the p53 C-terminal domain. *Cell* **90**, 595-606 (1997).
33. Gu, W., Shi, X. & Roeder, R.G. Synergistic activation of transcription by CBP and p53. *Nature* **387**, 819-823 (1997).
34. Harris, S. & Levine, A.J. The p53 pathway: positive and negative feedback loops. *Oncogene* **24**, 2899-2908 (2005).
35. Luo, J. et al. Acetylation of p53 augments its site-specific DNA binding both in vitro and in vivo. *Proc Natl Acad Sci U S A* **101**, 2259-2264 (2004).
36. Davis, J.A., Takagi, Y., Kornberg, R.D. & Asturias, F.A. Structure of the yeast RNA polymerase II holoenzyme: Mediator conformation and polymerase interaction. *Mol Cell* **10**, 409-415 (2002).
37. Espinosa, J.M., Verdun, R.E. & Emerson, B. p53 functions through stress- and promoter-specific recruitment of transcription initiation components before and after DNA damage. *Mol Cell* **12**, 1015-1027 (2003).
38. Wriggers, W. & Birmanns, S. Using situs for flexible and rigid-body fitting of multiresolution single-molecule data. *J. Struct. Biol.* **133**, 193-202 (2001).
39. Johnson, K.M., Wang, J., Smallwood, A. & Carey, M. The immobilized template assay for measuring cooperativity in eukaryotic transcription complex assembly. *Methods Enzymol.* **380**, 207-219 (2004).
40. Baek, H.J., Kang, Y.K. & Roeder, R.G. Human Mediator enhances basal transcription by facilitating recruitment of transcription factor IIB during preinitiation complex assembly. *J Biol. Chem.* **281**, 15172-15181 (2006).
41. Ranish, J.A., Yudkovsky, N. & Hahn, S. Intermediates in formation and activity of the RNA polymerase II preinitiation complex: holoenzyme recruitment and a postrecruitment role for the TATA box and TFIIB. *Genes Dev.* **13**, 49-63 (1999).
42. Harauz, G. & van Heel, M. Exact filters for general geometry three dimensional reconstruction. *Optik* **73**, 146-153 (1986).